X-ray white beam topography of self-organized domains in flux-grown $BaTiO_3$ single crystals

D. Walker,[1] A. M. Glazer,[1,2] S. Gorfman,[3] J. Baruchel,[4] P. Pernot,[4] R. T. Kluender,[4]
F. Masiello,[5] C. DeVreugd,[6] and P. A. Thomas[1]

[1]*Department of Physics, University of Warwick, Coventry CV4 7AL, United Kingdom*
[2]*Department of Physics, University of Oxford, Oxford OX1 3PU, United Kingdom*
[3]*Department of Physics, University of Siegen, Siegen, Germany*
[4]*ESRF, 71 avenue des Martyrs, CS 40220, Grenoble Cedex 9, France*
[5]*PANalytical BV, Almelo, The Netherlands*
[6]*Department of Materials Science and Engineering, Virginia Polytechnic Institute and State University, Blacksburg, Virginia 24061, USA*

(Received 19 February 2016; revised manuscript received 1 June 2016; published 12 July 2016)

The phenomenon of self-organization of domains into a "square-net pattern" in single-crystal, flux-grown $BaTiO_3$ several degrees below the ferroelectric to paraelectric phase transition was investigated using *in situ* synchrotron x-ray topography. The tetragonal distortion of the crystal was determined by measuring the angular separation between the diffraction images received from 90° *a* and *c* domains in the projection topographs, and shows a rapid decrease towards 110 °C, the onset temperature for self-organization. The onset of self-organization is accompanied by bending of the {100} lattice planes parallel to the crystal surface, which produces a strain that persists up to and beyond the Curie temperature, where the crystal becomes cubic and the self-organized domains disappear. At the Curie point, the bending angle $\alpha_{100} = 8.1(\pm 0.3)$ mrad is at a maximum and corresponds to the radius of curvature of the surface being $16.3(\pm 0.6)$ mm.

DOI: 10.1103/PhysRevB.94.024110

I. INTRODUCTION

$BaTiO_3$ (BT) is one of the most well-known tetragonal ferroelectric materials and is incorporated in a wide range of devices from capacitors to photorefractive storage media [1,2]. Although BT has been researched extensively for 60 years or so, there remain features of this material that are poorly understood. One such phenomenon is the self-organization of the domains into a so-called "square-net pattern" in single-crystal material. This was first observed by Forsbergh [3] in 1949, using conventional polarized light microscopy. Whether or not flux-grown BT crystals, which have a platelike morphology, show the square-net pattern at room temperature varies from sample to sample—Forsbergh's original observation was made at room temperature. He accounted for the square-net arrangement and showed that the periodicity was twice the crystal thickness using purely geometrical arguments. He also inferred that this would result in the crystal plate becoming bent. Lambert *et al.* [4] observed that some crystals having unusually small tetragonality (measured by the c/a ratio) show self-organization at room temperature, whereas others, which they refer to as "ordinary" crystals, show sudden self-organization when heated to approximately 5 °C below the Curie temperature. They pointed out that the anomalously small tetragonality was connected to the presence of the square-net pattern of domains. However, they were unable to account either for the temperature of the self-organization or indeed for why the phenomenon should occur at all. Schilling *et al.* [5] have produced a phenomenological theory to explain why self-organization can occur well below the Curie point. It makes reference to an optical birefringence imaging experiment on flux-grown BT by their co-author Glazer, which showed the occurrence of a square-net pattern at around 111 °C (Fig. 1) both upon heating and cooling of the crystal reversibly through the Curie point at 120 °C. The crystal that is the subject of this paper is from the same batch and self-organizes at the same temperature.

Yoneda *et al.* [6] carried out x-ray topography at SPring-8 on BT doped with 0.5% Sr, which has low tetragonality and shows square-net self-organization at room temperature. The topographic images they presented show that the diffracted intensity pattern splits into "stripes" having a separation that corresponds to the periodicity of the square net. They also estimated the tetragonal strain $(c/a - 1)$ within a "square" of the net to be of order 10^{-4}. In a much earlier experiment by Bordas *et al.* [7], which was the first white beam topography experiment conducted on BT as a function of temperature, the presence of "stripes" in a high-temperature image was observed, but it was not connected in that publication with the formation of self-organized domains.

The aim of the present work is to explore the development of the self-organization in flux-grown BT as a function of temperature by using x-ray synchrotron white beam topography. By this means, we could study self-organization simultaneously with the measurement of the tetragonality upon heating and cooling through the Curie point. The results are interpreted using a model that combines both tetragonal and bending strains below the Curie temperature and also shows the existence of a residual bending strain above. The self-organization is shown to be associated with a collapse of the tetragonality (c/a ratio) at ∼111 °C in this sample.

It is important to understand that flux-grown and top-seeded grown $BaTiO_3$ are fundamentally very different. The flux-grown crystals, such as that used here, contain chloride or fluoride ions as impurities, and exhibit a Curie temperature close to 120 °C, whereas for the purer top-seeded crystals it is closer to 140 °C [8]. Furthermore, flux-grown BT crystallizes in yellowish plates, while the top-seeded crystals are formed as near-colorless blocks. The self-organization observed by Forsbergh and others was seen in the flux-grown crystals, whereas this has not been observed in top-seeded crystals to our knowledge. It is not generally appreciated that considerable care has to be taken in making use of the measured physical

properties of BT derived from the literature, as until the 1960's most of them were obtained using impure flux-grown crystals.

II. EXPERIMENT

The flux-grown crystal used in this study was grown in Bell Labs in the late 1940's and was part of the collection of the late Dr. Helen D. Megaw. It is strongly tetragonal at room temperature. The crystal, which was approximately 300 μm thick, was examined using optical birefringence microscopy [9] (Fig. 1) to confirm that the self-organization occurred on heating at 110.6($\pm$0.5) °C. At room temperature the birefringence orientation image showed that the sample consisted of many laminar 90° domains.

The *in situ* white beam x-ray topography experiment was carried out at the BM05 imaging beamline at the ESRF. The flat ⟨001⟩-oriented $BaTiO_3$ crystal plate was polished to an optical finish of thickness 130($\pm$5) μm. The BT crystal was placed in a custom-built furnace [10] specifically designed for topographic imaging. The lower half of the crystal was sandwiched between two 150 μm Si wafers to provide good thermal contact and thus achieve a temperature gradient across the sample of $<$1°C/mm. Figure 2(a) shows the experimental arrangement. With respect to a Cartesian reference frame x,y,z, the x-ray beam was directed along x with the x-z plane horizontal. The crystal plate was tilted around the vertical y axis through 18.6°. The crystal was then heated into the cubic phase ($T > 130$ °C) and a transmission Laue photograph was recorded for the purposes of indexing the observed reflections. We studied the reflections in the horizontal x-z plane as this would greatly simplify the later analysis and assist with the indexing. With this in mind, the camera was positioned to optimize the recording of a strong {120}-type Bragg reflection. Note that the same reflection could be indexed as any of

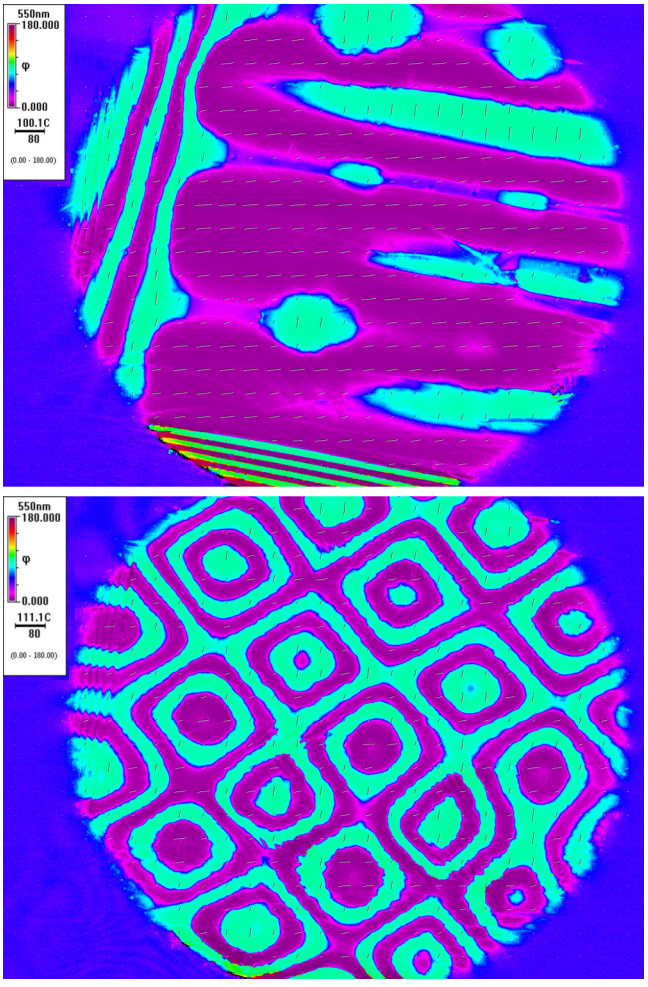

FIG. 1. Birefringence orientation images of flux-grown BT at (a) 100 °C and (b) 111 °C showing the effects of laminar and self-organized domains, respectively. The two colors (turquoise and purple) represent orientations of the optical indicatrix that are at 90° to each other. Zero degrees in orientation (purple) refers to the fast direction being approximately horizontal. Further details are provided in the companion paper by Schilling *et al.* [5]. The horizontal scale bar in the top left panel denotes a distance of 80 μm. The markers indicate the directions of the fast axes.

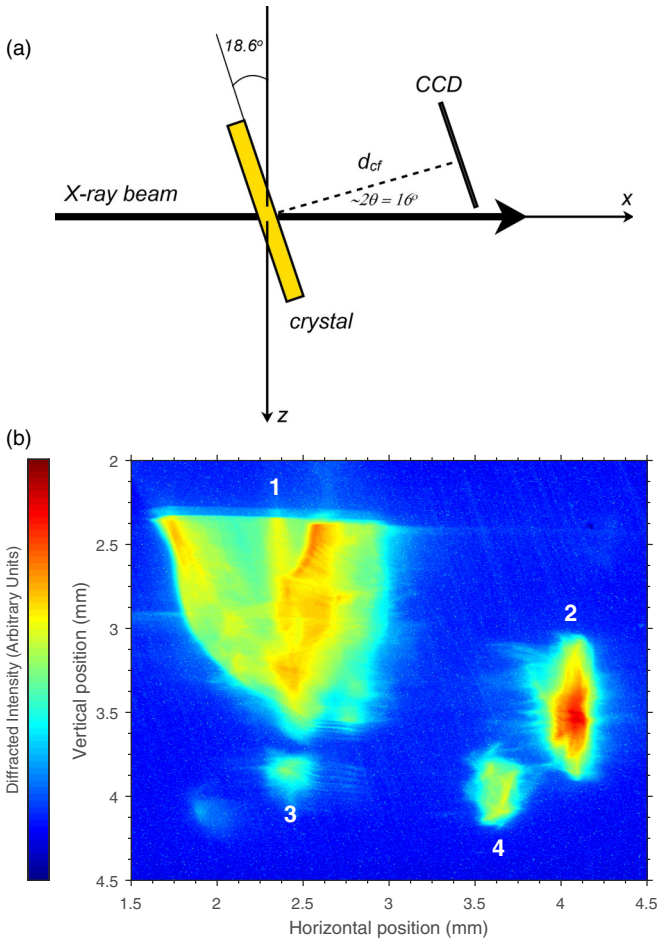

FIG. 2. (a) Schematic diagram showing experimental arrangement from above with respect to Cartesian axes x,y,z. The y axis points perpendicular to the page towards the viewer, and x-z is the horizontal plane of the experiment. (b) Projection topograph of the {120}-type reflections at 90°C. Spots 1 and 2 arise from the presence of 90° twin domains. Spots 3 and 4 are a result of mosaic spread and remain distinct from each other as the temperature is raised. By measuring the separation of these two spots with temperature, the change in tetragonality can be determined up to the onset of self-organization.

its other 23 variants of {120} in the cubic phase. Projection topographs of this reflection were then recorded between 90 °C and 135 °C using a FReLoN CCD camera (2045 × 2048 pixels per chip, with optics designed to give a 3 μm pixel size) placed at a crystal-to-detector plane distance d_{cf} of 24(±0.5) cm and tilted about the vertical y axis so as to be approximately perpendicular to the diffracted beams of interest. The sample was heated at a rate of 0.4 °C/min from 90 to 110 °C and then at 0.2 °C/min from 110 to 135 °C. Images were captured at 0.5 °C intervals in temperature.

III. RESULTS

A. Temperature region 1: from 90 to 110.5 °C

At 90 °C the {120} topograph is split into four Bragg peak components [Fig. 2(b)]. The two higher-intensity larger-area spots, marked as 1 and 2 on the figure, arise from the presence of 90° twin domains and must be assigned to two of the three reflections of type 201, 210, or 102, which all correspond to different d spacings and diffract at different angles (as shown in Fig. 3). The two lower-intensity components, marked as 3 and 4, result from a mosaic spread: Each of the two twin domains has two distinct orientations giving rise to the four spots. The positions of the small-area components, 3 and 4, were used to measure the diminishing separation of the twin reflections as a function of temperature. This is because they remain more distinct from each other as the temperature is raised compared with the upper pair, which merge into each other sooner simply because of the large area of spot 4. Although the wavelengths selected by the two sets of planes giving rise to spots 3 and 4 are not known, we are still able to calculate the angle between the normals to these planes from the positions of the spots,

$$\Delta\psi \sim \frac{1}{2}\left(\frac{\Delta D}{d_{cf}}\right)\cos^2 2\theta, \tag{1}$$

where ΔD is the distance between spots 3 and 4 measured from the topograph, 2θ is the mean scattering angle for the pair of spots, and the term $\cos^2 2\theta$ corrects for the obliquity.

It is therefore possible to derive the tetragonal (c/a) ratio of the crystal from the separation of the spots as follows. In the tetragonal system, $a = b \neq c, \alpha = \beta = \gamma = 90^\circ$. For BT, three 90° domain configurations can exist, which differ from one another by the orientation of their polar axis $\boldsymbol{c}$, relative to the crystal faces. We designate these three 90° domains as the X, Y, and Z domains, correspondingly. The following reciprocal lattice vectors $\boldsymbol{H}_X, \boldsymbol{H}_Y$, and $\boldsymbol{H}_Z$ [Fig. 3(a)] give rise to the Bragg reflections, arising from the X, Y, and Z domains,

$$\begin{aligned} \boldsymbol{H}_X &= 2a^*\boldsymbol{x} + c^*\boldsymbol{y}, \\ \boldsymbol{H}_Y &= 2c^*\boldsymbol{x} + a^*\boldsymbol{y}, \\ \boldsymbol{H}_Z &= 2a^*\boldsymbol{x} + a^*\boldsymbol{y}, \end{aligned} \tag{2}$$

where $a^* = \frac{1}{a}$ and $c^* = \frac{1}{c}$ are the lengths of the reciprocal basis vectors. The angle φ_{nm} between any of these reciprocal lattice vectors pairs, n and m, is given simply by

$$\cos(\varphi_{nm}) = \frac{\boldsymbol{H_n} \cdot \boldsymbol{H_m}}{|\boldsymbol{H_n}||\boldsymbol{H_m}|}. \tag{3}$$

Taking into account the well-known formulas for scalar products, we obtain

$$\begin{aligned} \cos^2(\varphi_{XY}) &= \frac{(4T^* + 1)^2}{5(4T^{*2} + 1)}, \\ \cos^2(\varphi_{XZ}) &= \frac{25T^{*2}}{(4T^{*2} + 1)(T^{*2} + 4)}, \\ \cos^2(\varphi_{YZ}) &= \frac{(T^* + 4)^2}{5(T^{*2} + 4)}, \end{aligned} \tag{4}$$

where $T^* = a^*/c^* = c/a$. Equations (4) describe the angular separation between the diffracted beams given for any pair of domains in question. In the next step, we assign the spots 3 and 4 to two of the X, Y, or Z domains and define the c/a rate by comparing the observed separation with that predicted by Eqs. (4).

This assignment is made by analyzing the directions of the displacements of spots 3 and 4 during the temperature variation. Although the way that the tetragonal lattice parameters vary as BT approaches the Curie temperature is well known, detailed quantitative studies have seldom been reported in the literature. The most reliable values for the tetragonal strain with temperature close to the tetragonal to cubic phase transition are from x-ray powder diffraction data recorded by Megaw [11] (Fig. 4) and from single crystals by

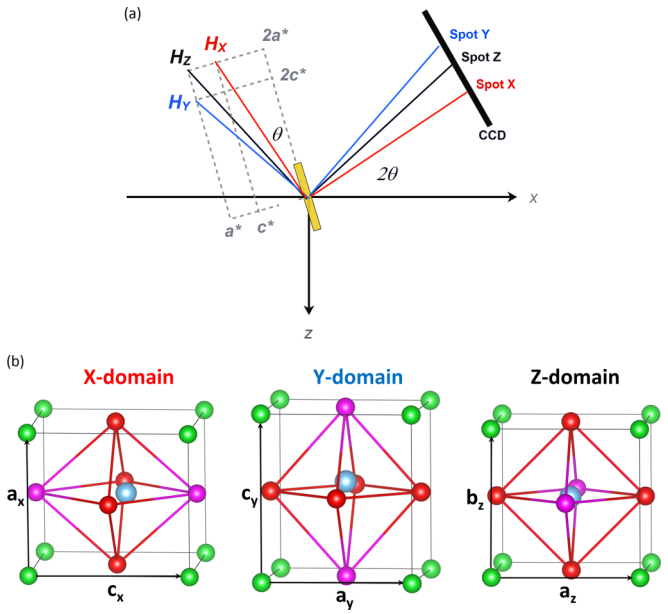

FIG. 3. (a) Schematic diagram of the reciprocal lattice vectors, giving rise to the {120} Laue spots from three different classes (X, Y, and Z) of tetragonal $BaTiO_3$ domains. For clarity, the diagram is not drawn to scale, but assumes $c > a$ (meaning that $c^* < a^*$), where c, a, c^*, and a^* are the corresponding direct and reciprocal tetragonal lattice parameters. The positions of the Laue spots on the detector are also indicated. (b) Schematic diagrams showing orientation of X, Y, and Z domains. The tetragonal polar axes of the domains are parallel and/or perpendicular to the crystal faces. Red and mauve spheres: oxygen; blue sphere: Ti; green spheres: Ba.

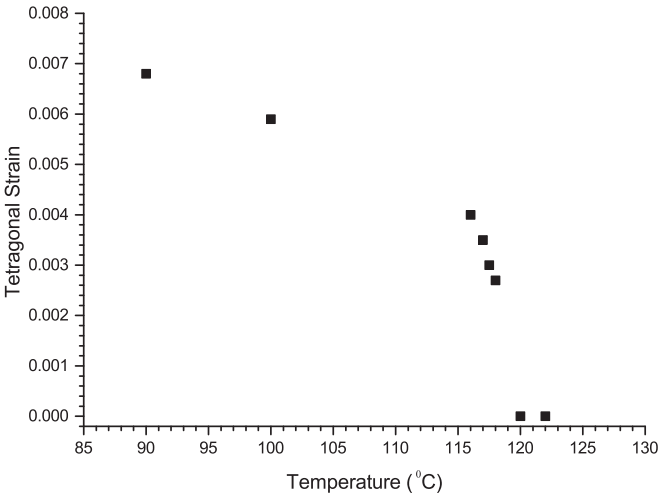

FIG. 4. Tetragonal strain derived from the lattice parameter measurements of Megaw [11]. These measurements were made on a crushed ceramic powder in which self-organization of the domains does not appear.

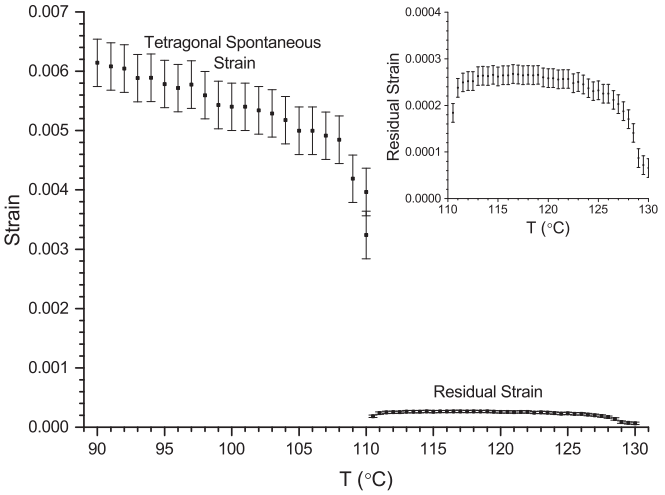

FIG. 5. Strain as a function of temperature. In the laminar region before the onset of self-organization close to 110 °C, this corresponds to the tetragonal spontaneous strain ($c/a - 1$) and is calculated from the angular separation of spots 3 and 4. The errors are computed from the error in measuring the separation on the film and that in the crystal to film distance. Above 110 °C, coinciding with the onset of self-organized domains, the tetragonality has become extremely small and this is now a residual strain (shown in the inset), calculated from the misorientation of the domains, which persists until ∼10 °C above the Curie point at 120 °C.

Clarke [8]. Both of these authors report that between 90 and 110 °C, the a ($= b$) lattice parameter increases with increasing temperature whereas c decreases at approximately the same rate. Accordingly, the reciprocal lattice parameters a^* ($= b^*$) decrease with increasing temperature, whereas c^* increases. Denoting the relative change in a^* and c^* as $-\Delta^*$ and Δ^*, respectively, we can predict how the Bragg angles of the Laue spots arising from the X, Y, and Z domains would change. It follows from Fig. 3(a) that the Bragg angles are given by

$$\tan\theta_X = \frac{1}{2}\frac{c^*}{a^*}\tan\theta_Y = \frac{1}{2}\frac{a^*}{c^*}\tan\theta_Z = \frac{1}{2}. \quad (5)$$

Assuming that Δ^* and $\Delta\theta$ are small, and using a first-order Taylor expansion, we find that $\tan(\theta + \Delta\theta) = \tan\theta + \frac{\Delta\theta}{\cos^2\theta}$ and $\frac{1+\Delta^*}{1-\Delta^*} = 1 + 2\Delta^*$. Therefore, we obtain the following expressions for the displacements of the Laue spots:

$$\Delta\theta_X = \cos^2\theta\frac{c^*}{a^*}\Delta^*, \quad \Delta\theta_Y = -\cos^2\theta\frac{a^*}{c^*}\Delta^*, \quad \Delta\theta_Z = 0. \quad (6)$$

Table I summarizes these results, showing that while the Z spot should not move, X and Y spots (if present) should move in the opposite directions, both approaching the Z spot. As shown in the video in the Supplemental Material [12], when the temperature is increased, spot 4 moves to the left (decreasing Bragg angle) towards spot 3, while spot 3 remains stationary. This unequivocally assigns spot 4 to the Y domain and spot 3 to the Z domain. Therefore, the angle between them corresponds to φ_{YZ} and the tetragonal strain is solved from Eqs. (4).

TABLE I. The position of {120} Bragg reflections from X, Y, and Z domains and their displacement across the topograph on the assumption that the c axis decreases with temperature at approximately the same rate as the a axis increases. Δ^* denotes the relative change of the reciprocal basis lengths, $a^* \to a^*(1 - \Delta^*)$ and $c^* \to c^*(1 + \Delta^*)$.

	X domain	Z domain	Y domain
$\tan\theta$	$\frac{1}{2}\frac{c^*}{a^*}$	$\frac{1}{2}$	$\frac{1}{2}\frac{a^*}{c^*}$
$\Delta\theta$	$\cos^2\theta\frac{c^*}{a^*}\Delta^*$	0	$-\cos^2\theta\frac{a^*}{c^*}\Delta^*$

Figure 5 shows the tetragonal strain calculated from the angular separation φ_{YZ} as a function of temperature between 90 and 110.5 °C (the onset of self-ordering) using Eq. (5). A sharp decrease in the tetragonal strain is observed at the onset of self-organization at 110.5 °C. We note that the magnitude of the tetragonal strain that we have derived from our measurements at 90°C is $c/a - 1 = 0.0062(\pm 0.0005)$, which is comparable to the value of 0.0068 derived from Megaw's work (plotted here in Fig. 4).

B. Temperature region 2: 110.5–135 °C

Above 110.5°C, it is no longer possible to distinguish the two diffraction spots corresponding to the 90° domains, which were used to measure the tetragonal strain in the previous section. However, the onset of self-organization in the crystal gives rise to a second effect which can be used to infer a bending strain. Figure 6 shows the {120} Laue topographs recorded at $T = 108$ and 115 °C, respectively. Whereas the image at 108 °C still shows the splitting between spots 3 and 4, the topograph recorded at 115 °C, which is in the region of self-organization, has significantly expanded in width W. (This sudden expansion is very evident in real time in the video.) Forsbergh noted in his paper that triangular prisms of 90°-oriented domains in the self-organized region should give rise to a curvature of the surfaces of the crystal [3]. The expansion of the topographic image that we have observed here is proof that this surface curvature indeed occurs, as only a bending

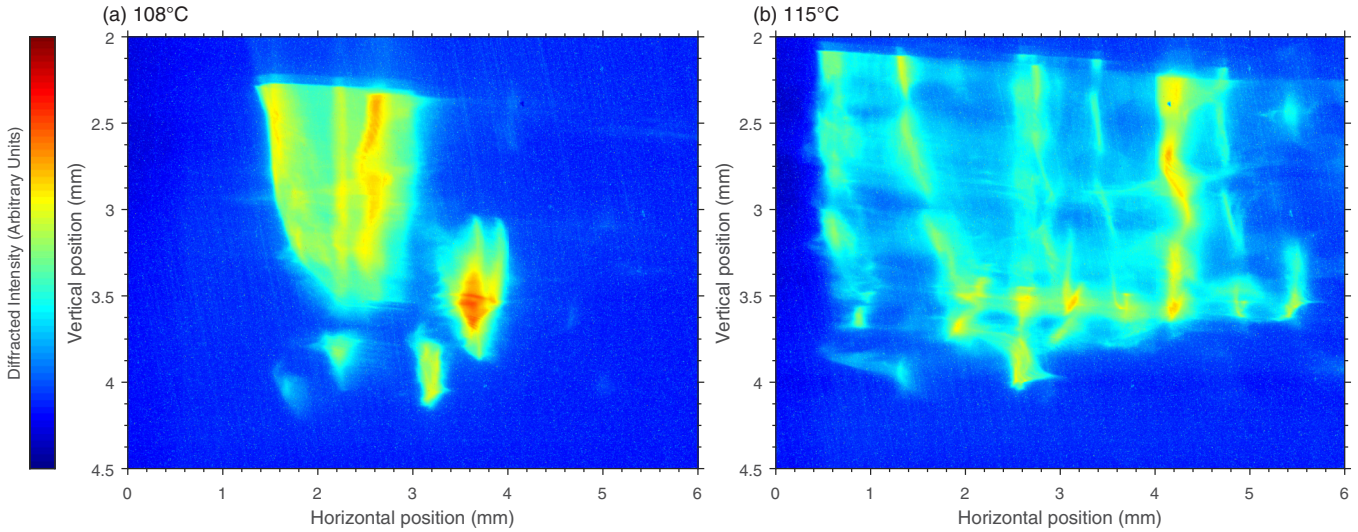

FIG. 6. {120} projection topographs at (a) 108 °C and (b) 115 °C. The self-organization of the domains manifests itself as an increase of the topographic width compared with the case where only laminar domains are present.

of the near-surface planes would give a physical expansion of the topograph's width, as explained by Walker *et al.* [13] with respect to a similar observation in the material $RbTiOAsO_4$ when subjected to an applied electric field. We also note that the topographic image is crossed by a number of quasiperiodic high-intensity stripes in the vertical direction. These areas of the crystal diffract more strongly than the rest, suggesting that they are regions of higher strain. In the kinematic theory of diffraction, an area of higher strain has a larger range of d spacings than in dynamical scattering from a perfect crystal. The wider range of d spacings can achieve the Bragg condition from a wider selection of wavelengths in the white beam. Hence, a high-strain region, e.g., resulting from a dislocation, appears as a region of black (high intensity) against the low intensity of the rest of the (more) perfect crystal.

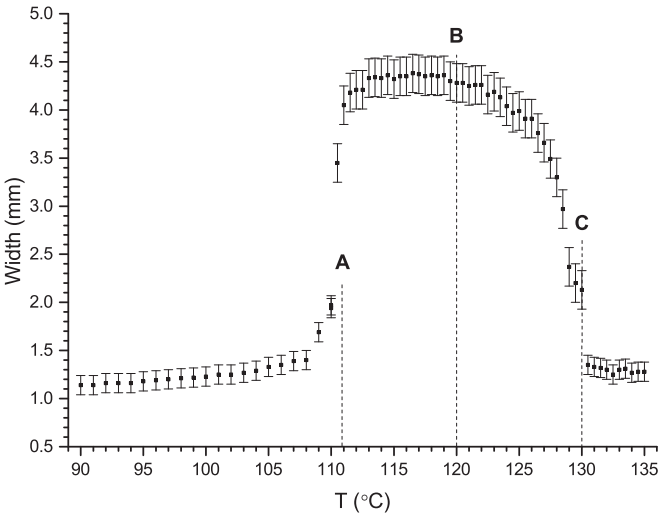

FIG. 7. Measured width of {120} projection topographs. A: Onset of self-organization. B: Curie point. C: Removal of bending. The errors are from the uncertainty in measuring the widths on the film.

Figure 7 shows the measured physical width of the {120} topograph as a function of temperature. From 90 to 110 °C, the width increases slowly, an effect attributable to the normal thermal expansion of the crystal. The onset of self-organization at 110.5°C (A) is marked by a sudden fourfold increase in the width of the image, which then remains almost constant up to the phase transition (B), which had earlier been measured for this crystal by optical birefringence microscopy to be 120 °C. Above the phase transition, the width of the topograph begins to decrease, and at 130 °C (C) it returns to its value just prior to the self-organization event.

The dramatic increase in topographic width at 110.5 °C corresponds to the formation of the prismatic domains and resultant curvature of the crystal surface, which was first observed and explained by geometry in Forsbergh's original work. The topographic width and surface curvature attain their maxima at the Curie temperature (120 °C) where the lattice parameters a (=b) and c become truly equal and the intrinsic tetragonal strain goes to zero. At this point, in the optical birefringence imaging experiment, which is in transmission through the crystal and is insensitive to surface curvature, the self-organized pattern disappears. In this x-ray topography experiment, however, we observe that the effect of the self-organization in producing surface curvature does not disappear as soon as the Curie point is attained. This observation is consistent with the comment by Forsbergh that bending of the crystal persists beyond the Curie point, although he was not able to quantify its magnitude or the temperature range. If the crystal is still bent, this implies either (a) that there is a remanent internal strain caused by a trace (the "history") of the prismatic domains even in the cubic phase where $c/a = 1$, or (b) that regardless of the presence or absence of prismatic domains (or their trace), the macroscopic bending of the crystal surfaces requires a further input of thermal energy to relax. Hence, the crystal has to be heated by a further 10 °C to restore the surface to its original unbent state. We have observed that on cooling, the width of the topographic image suddenly increases at about 126 °C, and then levels off at the Curie point,

finally decreasing to a minimum at about 110 °C. This suggests that the mechanism for the bending in the high-temperature phase is connected to having a remanent internal strain rather than simply being caused by thermal relaxation.

The radius of curvature of the {100} planes (parallel to the surface) is deduced from the observed increase in width of the {120} projection topographs in the self-organized region, compared with the width of 1.4(±0.1) mm just before the onset of self-organization at 108 °C. The topographic width attains its maximum value of 4.3(±0.2) mm within the temperature range 115–122 °C. This gives an expansion of the topograph ΔW of 3.0(±0.2) mm. As both surfaces expand equally in the topographs, the bending angle of the planes, α_{210}, is given simply by $\Delta W/4d_{cf}$ [14], from which $\alpha_{210} = 3.0(\pm 0.1)$ mrad. The fact that the topographic image expands means that the curvature is in the convex sense as seen along the direction of the x-ray beam. For the {100} planes, $\alpha_{100} = 1.42(\pm 0.05)$ mrad and the radius of curvature of the surface ($2\alpha_{100}$) is 2.8(±0.1) mm. Therefore, the misorientation of these planes causes a longer surface at the bases of the prisms. The extension is given by

$$\Delta S = L \tan(\alpha_{100}) = 0.18(\pm 0.02)\ \mu\text{m}, \tag{7}$$

where L is the thickness of the crystal (130 μm). The strain $\Delta S/S$ (where S is half the original width of the sample surface, as estimated from the observed width of the topograph at 108 °C before self-organization appears) is related to the difference in d spacing between the two sets of 90°-oriented domains. Therefore, the residual strain at 115 °C is measured to be $0.000\,26(\pm 2 \times 10^{-5})$. This can be compared with the much larger strain observed by Clarke [8] of 0.0076 for flux-grown BT and 0.0050 for top-seeded crystals at this same temperature. It appears then that when self-organization occurs, the spontaneous strain approaches close to zero compared with that observed for normal behavior. This effect was also observed by Lambert *et al.* [4]. Figure 5 shows the residual strain as a function of temperature across the entire measured temperature range from 90 to 135 °C.

IV. CONCLUSIONS

An *in situ* x-ray white beam topography experiment was performed on a {100} flux-grown BT single crystal. The tetragonal strain as a function of temperature was determined up to the appearance of self-organized domains at 110 °C by measuring the separation of two diffraction spots corresponding to two separate 90° laminar domains with diffraction maxima (spots). The measured tetragonal strain agrees well with the published literature below the self-organization temperature, which was determined from this study to be 110.5 °C, in close agreement with earlier optical studies on the same batch of crystals. Our results show a dramatic decrease in tetragonality at the onset of self-organization, which agrees with the previous ideas of Lambert *et al.* and Yoneda *et al.* The onset of self-organization is shown to correspond to a sudden surface curvature (evidenced by an increase ΔW in the width of the topographs), in agreement with the original idea of Forsbergh, and we have determined that at its maximum, this curvature corresponds to a misorientation of the {100} planes parallel to the surface of ∼1.4 mrad. This maximum of the curvature appears at the Curie point (120 °C) and then decreases to the original unbent state of the surface at 10 °C above this temperature (130 °C). As a result of this experiment, therefore, we have been able to follow and separate two types of strain intrinsic to BT, i.e., the tetragonal strain as a function of temperature and the surface strain due to the formation of prismatic self-organized domains, which gives rise to curvature of the surfaces. It is observed that just above the Curie point, where $c/a = 1$ and the intrinsic tetragonal strain is zero, there remains a surface-bending strain of comparable magnitude with that existing just above 110.5 °C, which gives rise to the sustained large width of the expanded topograph. We therefore infer that after the onset temperature for self-organization, the dominant effect is primarily the surface bending strain, with the tetragonal strain (which we have already commented is anomalously low compared with Megaw's powder diffraction measurements, for example) contributing less than 10% of the observed effect. The observation that the bending reappears above the Curie point on cooling suggests that the bending is caused by a remanent strain and can be thought of as a memory effect.

In the companion paper by Schilling *et al.*, it is explained why the self-organization appears in flux-grown barium titanate and why it occurs so suddenly just below the phase transition temperature. Further work is needed to explain why this effect does not occur in purer top-seeded crystals. There is currently a considerable amount of theoretical research being carried out on domain formation in ferroelectric materials such as barium titanate, and this should lead to a fuller understanding of why the domains form and in which arrangements. For instance, the application of compressive strains on thin films of barium titanate has been shown to give rise to intriguing domain patterns that do show the kind of complexity seen in the flux-grown crystals [15,16].

[1] G. H. Haertling, J. Am. Ceram. Soc. **82**, 797 (1999).

[2] D. Kip, Appl. Phys. B: Lasers Opt. **67**, 131 (1998).

[3] P. W. Forsbergh, Jr., Phys. Rev. **76**, 1187 (1949).

[4] M. Lambert, A. M. Quittet, C. Taupin, and A. Guinier, J. Phys. (Paris) **25**, 345 (1965).

[5] A. Schilling, A. Kumar, R. G. P. McQuaid, A. M. Glazer, P. A. Thomas, and J. M. Gregg, preceding paper, Phys. Rev. B **94**, 024109 (2016).

[6] Y. Yoneda, J. Mizuki, Y. Kohmura, Y. Suzuki, S. Hamazaki, and M. Takashige, Jpn. J. Appl. Phys., Part 1 **43**, 6821 (2004).

[7] J. Bordas, A. M. Glazer, and H. Hauser, Philos. Mag. **32**, 471 (1975).

[8] R. Clarke, J. Appl. Crystallogr. **9**, 335 (1976).

[9] A. M. Glazer, J. G. Lewis, and W. Kaminsky, Proc. R. Soc. London, Ser. A **452**, 2751 (1996).

[10] P. Pernot, B. Gorges, H. Vitoux, R. Kluender, F. Masiello, and J. Baruchel, Phys. Status Solidi A **206**, 1880 (2009).

[11] H. D. Megaw, Proc. R. Soc. London, Ser. A **189**, 261 (1947).
[12] See Supplemental Material at http://link.aps.org/supplemental/10.1103/PhysRevB.94.024110 for video showing the change in the {120} topograph as a function of temperature from 90 °C up to 135 °C.
[13] D. Walker, P. A. Thomas, P. Pernot-Rejmankova, and J. Baruchel, J. Appl. Crystallogr. **40**, 505 (2007).
[14] D. Walker, P. A. Thomas, Q. Jiang, P. Pernot-Rejmankova, J. Baruchel, and T. Ayguavives, J. Phys. D: Appl. Phys. **38**, A55 (2005).
[15] L. Q. Chen. J. Am. Ceram. Soc. **91**, 1835 (2008).
[16] Y. L. Li and L. Q. Chen, Appl. Phys. Lett. **88**, 072905 (2006).